Insect monitoring with fluorescence lidar techniques: feasibility study

Mikkel Brydegaard,[1,*] Zuguang Guan,[1] Maren Wellenreuther,[2] and Sune Svanberg[1]

[1]Atomic Physics Division, Lund University, P.O. Box 118, SE-221 00 Lund, Sweden

[2]Department of Ecology, Lund University, SE-223 62 Lund, Sweden

*Corresponding author: mikkel.brydegaard@fysik.lth.se

Received 22 July 2009; revised 27 September 2009; accepted 27 September 2009; posted 28 September 2009 (Doc. ID 114651); published 12 October 2009

We investigate the possibilities of light detection and ranging (lidar) techniques to study migration of the damselfly species *Calopteryx splendens* and *C. virgo*. Laboratory and testing-range measurements at a distance of 60 m were performed using dried, mounted damselfly specimens. Laboratory measurements, including color photography in polarized light and spectroscopy of reflectance and induced fluorescence, reveal that damselflies exhibit reflectance and fluorescence properties that are closely tied to the generation of structural color. Lidar studies on *C. splendens* of both genders show that gender can be remotely determined, especially for specimens that were marked with Coumarin 102 and Rhodamine 6G dyes. The results obtained in this study will be useful for future field experiments, and provide guidelines for studying damselflies in their natural habitat using lidar to survey the air above the river surface. The findings will be applicable for many other insect species and should, therefore, bring new insights into migration and movement patterns of insects in general.

OCIS codes: 280.3640, 010.1100, 300.2530, 350.4238, 240.5698, 030.1670.

1. Introduction

A. Background

Light detection and ranging (lidar) techniques have been developed for almost half a century and have since been widely used in, e.g., aerosol monitoring [1–6]. Stationary lidars and mobile systems have been employed with a wide variety of platforms, ranging from submarines, ships, trucks, cranes, airplanes, to satellites [7–10]. Aerosol studies typically involve vertical soundings or the generation of three-dimensional distribution maps. The data are usually obtained by time-resolved measurements of elastic backscattering using a limited number of laser frequencies. Even polarization of backscattered light can be analyzed to provide information regarding the number of scattering events and particle size distribution [10,11]. Apart from the strongly dominating elastic backscattering methods, three further lidar methods have been developed for detailed spectral analysis and classification of aerosols. These methods are based on (laser-induced fluorescence (LIF) spectroscopy [12–16], Raman spectroscopy [17], and laser-induced breakdown spectroscopy (LIBS) [18–22]). LIF methods have been employed in the past to distinguish between different types of pollen and aerosols that can potentially be used in biological warfare [16]. Raman lidar gives weak signals and has mostly been employed on water and nitrogen [17]. The LIBS method is more difficult to employ, but recent work has demonstrated assessment of aerosol salinity [22], following very early Russian work on cement particles [18]. Traditionally, aerosol particles are considered to be solid or liquid particles that can range from smoke, which has a particle size of a few nanometers, to friction particles and raindrops of several hundred micrometers in size. In addition to these advances, insects and even vertebrates, such as birds and bats, could potentially be detected using lidar techniques. In the past, bird

0003-6935/09/305668-10$15.00/0

and insect monitoring and tracking have been excessively investigated using radar methodologies [23–26], including the classification of animals by multiband (matched) illumination [27,28]. Such applications of remote sensing techniques have important implications for local agriculture, as they allow pest forecasting. Reflectance signatures measured with multiband radar methods are typically given by interference arising from the structures of the reflecting object. However, similar advances in the use of lidar techniques have been slow, and until now, only a few studies have directly investigated the feasibility of lidar in insect and vertebrate monitoring. One example comes from a lidar study on honey bees in land mine detection [11]. That study measured backscattered light at a single wavelength and in two polarizations to detect bee echoes and to build up stochastic histograms to summarize the bee concentration in relation to the actual land mine locations. In addition, lidar sounding of fish demonstrated the possibility to detect moving live scatterers [29,30]. The bee study was followed up by investigations involving background rejection by wing beat modulation of reflected light [31,32]. Such an approach has also been used in the bird radar community [33], with the difference that the modulation frequencies are several magnitudes smaller.

B. Motivation and Strategy

The present paper describes spectroscopic studies of two odonate species (Odonata: damselflies and dragonflies), the banded demoiselle *Calopteryx splendens* and the beautiful demoiselle *C. virgo* [34]. In particular, the main focus of this study was to test the feasibility of lidar for damselfly monitoring and study of movement patterns. Damselfly larvae are highly sensitive to water pollution and oxygen concentrations and have thus been used as biomarkers in the past [35]. Another important characteristic of damselflies is that, like all other insects, they are ectotherms and are particularly sensitive to changes in temperatures. Therefore, increasing ambient temperatures are expected to force insect species to shift their distributions by expanding into new geographic areas and by trying to escape from areas that become climatically unsuitable [36]. In Europe, many documented cases of range shifts among insects have been attributed directly to increasing temperatures [37]. For example, out of the 35 European butterfly species that were studied [38], 22 have shifted their ranges northward by 35–240 km over the last century, whereas only two have shifted south. There is also direct evidence that the species studied in the present work, *Calopteryx splendens* and *C. virgo*, are currently affected by climate change. In a recent study [39] Hickling *et al.* showed that 23 of the 24 temperate Odonata species in the United Kingdom, including the two *Calopteryx* species, significantly expanded their range size and northern range limit between 1960 and 1995. Together, these data strongly indicate that European populations of these insects are currently moving northward.

Migration studies of insects are crucial for understanding the roles of gene flow in connecting population over a wide spatial scale [40,41], but progress in this area has been hampered by the difficulty of marking individuals. As a consequence, studies typically involve neighboring and low numbers of populations. Migration in insects is relatively difficult to study with traditional methods, such as radio transmitters or light loggers, because the size and weight of damselflies makes the attachment of the disproportionately large devices difficult. An alternative approach would be to mark neighboring populations with combinations of two or three different fluorescent dyes, such as Rhodamine variants, and then detect migrated marked individuals at a given population [42], by correlating the spectral fingerprint of each detected individual with the population of origin. Such dyes could either be sprayed or powdered on individual specimens or absorbed by the individual through the metabolic uptake of food or water (e.g., during the aquatic larval stage) [42–46]. A number of fluorescent dyes have already been used for freshwater tracking and environmental studies, and other dyes already exist due to detergents in wastewater [47]. Even with only a few appropriate and noninterfering dyes, a much larger number of site locations could be monitored simultaneously by using various nonparallel spectral combinations of the few dye types. This is especially true if the probability of detecting two individuals in a single voxel is small.

This paper presents optical spectroscopic features and the feasibility of damselfly monitoring using lidar and lidar LIF methods, and is organized in the following way. In Section 2 the general photophysical aspects of Odonata are discussed. Then, in Section 3, we develop strategies for the remote classification of the two damselfly species and the respective genders in order to produce species and gender selective three-dimensional distributions and behavioral studies over a temporal scale [48]. In particular, we demonstrate how to generate broadband “white” light by autofluorescence on the surface layers of *C. splendens* and *C. virgo* in order to detect how structural colors affect fluorescence. Such surface probed fluorescence studies have resemblance to those presented in [49]. In addition, laboratory and outdoor test range measurements are also described, including descriptions of methods for damselfly marking [42] to study migration of individuals between populations. For this we further investigate lidar LIF methods enhanced by fluorescent dye marking. In the latter case, individuals are marked with dye either by spraying or powdering dyes directly on the individual [46] or by adding dyes to the water, which is then incorporated into the body by the individual during the larval phase [50]. We further show how the structural imprint of the dye-enhanced fluorescence can be used for remote classification

of species and genders. Finally, in Section 4, we discuss the results and give suggestions for future work.

2. Damselfly Species Description and Relevant Photophysics

Photographs of *Calopteryx splendens* and *C. virgo* of both genders are shown in Fig. 1. The optical properties of the majority of insects are determined both by the chemical absorption imprint yielding "classical" colors, and structural colors, due to interference [51–58]. This becomes particularly clear when damselflies are observed in polarized light [58]. While common lidar methods like LIF lidar, differential absorption lidar (DIAL), and LIBS lidar commonly measure chemical colors, structural colors have never been measured in the lidar community, due to the fact that organized cells or organelles and layered structures on the nanoscale are required for the effect to be noteworthy. Even though ordinary cells might leave weak structural imprints in traditional reflectance, absorption, or fluorescent measurements [59,60], such effects are typically neglected. The main features of the reflectance of the damselfly abdomen can be explained by the arrangement of approximately 100 nm sized scattering nanospheres. (This is illustrated in Fig. 7(c) adopted from [61], to be discussed later.) This arrangement provides damselflies with their typical retroreflective properties, and an approximately 100 nm broad reflection band shifting from the blue to the green region, depending on the sizes of the nanospheres and on the angle of observation with respect to surface orientation and illumination. The nanosphere arrangement is situated just below the chitin cuticulum; the cuticulum can be more or less melanized [62]. Both chitin and melanin absorption peaks around 330 nm and both chitin and melanin produce broad fluorescence spectra covering the structural features in the blue and green region [63–65]. Further, certain Ordonates are known to have wax covered wings [66]. Botanical waxes are well studied in LIF lidar [67]. Typically, wax absorption increases dramatically below 355 nm and the maximum fluorescence yield is usually obtained around 330 nm excitation. Even waxes provide broad fluorescence spectra peaking in the blue region [68]. Reflectance can be further modified by absorbing ommochrome granules, which are situated beneath the scattering arrangement and prevent nonscattered light from being reemitted and, thus, strengthen the structural color. Furthermore ommochromes in certain Odonata species react to the temperature, regulating the temperature of the ectotherms by either migrating into the nanosphere region or contracting to a deeper lying layer, which increases reflectance. Such effects can be expected to alter even the fluorescence. The lowest of the six visual spectral bands typically found in Odonata [69] goes as far as 350 nm in the UV; thus, it is not unreasonable to expect the studied species to sexually signal via altered reflectance in this band. Vibrant structural colors are exhibited by the blue males of *C. splendens* and the green males of *C. virgo* [70]. Females of both species appear less colorful, with brown, green, and golden shadings. Males and females of the two *Calopteryx* species differ significantly in the absorption properties of their wings, due to differences in the amount of melanin. Males of *C. virgo* typically have over 90% of their wings melanized, whereas males of *C. splendens* have melanized patches covering about 50% of the wing surface [71–74]. Females of both species lack the melanized wing patches, but *C. virgo* females are brown, while *C. splendens* females are typically green [50].

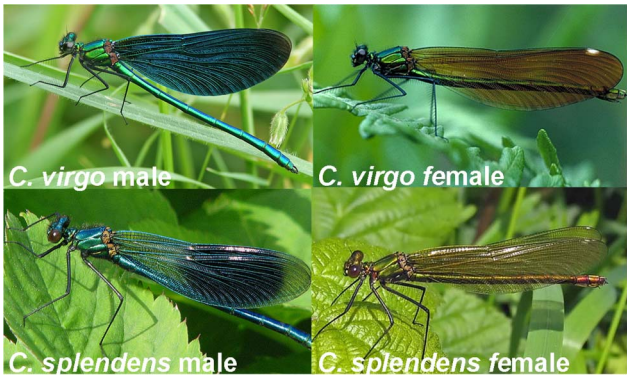

Fig. 1. (Color online) Males of *C. virgo* have almost completely melanized wings, whereas males of *C. splendens* have melanized wing patches. The wings of *C. virgo* females are brown, while the wings of *C. splendens* females are typically green.

3. Methods, Measurements, and Results

Optical measurements were performed under controlled conditions, both on a macro scale in the laboratory and on a 60 m lidar testing range. Measurements were taken in order to gain insights into the optical properties of the studied species and to develop realistic and practical methods for future field work.

A. Laboratory Measurements

The reflective properties caused by the structural colors were investigated in detail in the laboratory. To confirm that the blue and green shades are indeed structural, two samples were photographed from a distance of 60 cm with a Sony F828 digital still red-green-blue (RGB) camera with a fixed visible linear polarizing laminated film (Edmund Optics) attached to the objective. The sample was illuminated by collimated light from a filament source (100 W Oriel, halogen–tungsten blackbody source) at an angle of 15°; see Fig. 2. For the experiment, two dried specimens (*C. splendens*, male and female) were fixed on a wire, and were photographed with parallel and perpendicular polarized illumination with respect to the polarizer on the camera objective. The photographs with maintained polarization reveal green, golden, and blue shades (Fig. 3), whereas the depolarized pictures are considerably darker and show mostly brown and reddish colors. For the convenience of the viewer, the intensities of the depolarized

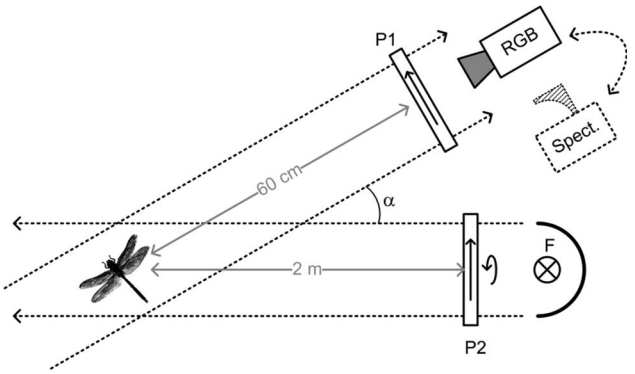

Fig. 2. Setup for color imaging and whole-body polarized reflectance studies. Samples are observed either with a color camera (RGB) or a spectrometer (Spect.) at low angle ($\alpha = 15°$) through a linear polarizer (P1). Collimated white illumination is provided by a tungsten filament lamp (F) which can be polarized in parallel or perpendicularly to P1 using P2.

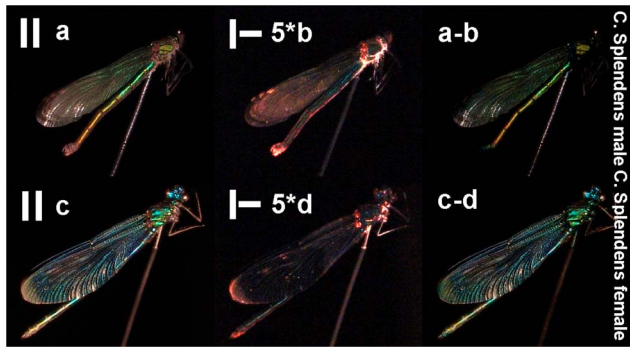

Fig. 3. (Color online) Photograph of damselflies in polarized light. Photographs a and c, indicated with ||, are photographed with parallel polarizers. Photographs b and d, indicated with ⊢, show the depolarized light amplified by a factor of 5 to make it visible to the reader. Subtraction gives us the two figures to the outermost right, where structural colors remain.

photographs in Fig. 3 are multiplied by a factor of 5. Depolarized reflections originate mainly from the hairy parts of the specimens, more specifically, from multiple reflections of the four-folded wing and the abdomen tip. By subtracting the depolarized intensity from the polarized, we retain the pure structural color and, again, green, golden, and blue shades are observed. This finding is in contrast to the appearance of multiple-scattering biological samples, such as leaves or skin, where the structural color appears flat white, simply describing the refractive index of the sample (specular reflex). Following that, the samples were studied in a stereo microscope with a ring light configuration, and the results showed that the structural blue and green shades were distributed over the entire body and wings, despite the fact that the effect to the naked eye was most obvious on the abdomen and thorax.

Studies of the whole-body reflectance were also performed by exchanging the RGB camera with a spectrometer (Ocean Optics USB4000) with an off-axis parabolic mirror telescope; see Fig. 2. Again, the spectral reflectance of the polarized and depolarized lights were measured for both specimens (*C. splendens* males and females); see Fig. 4. The depolarized reflectance is more than 1 magnitude smaller than the polarized, and the blue and green structural imprint disappears. The units are referenced to a Ø 50 mm barium sulfate plug (approximately the size of

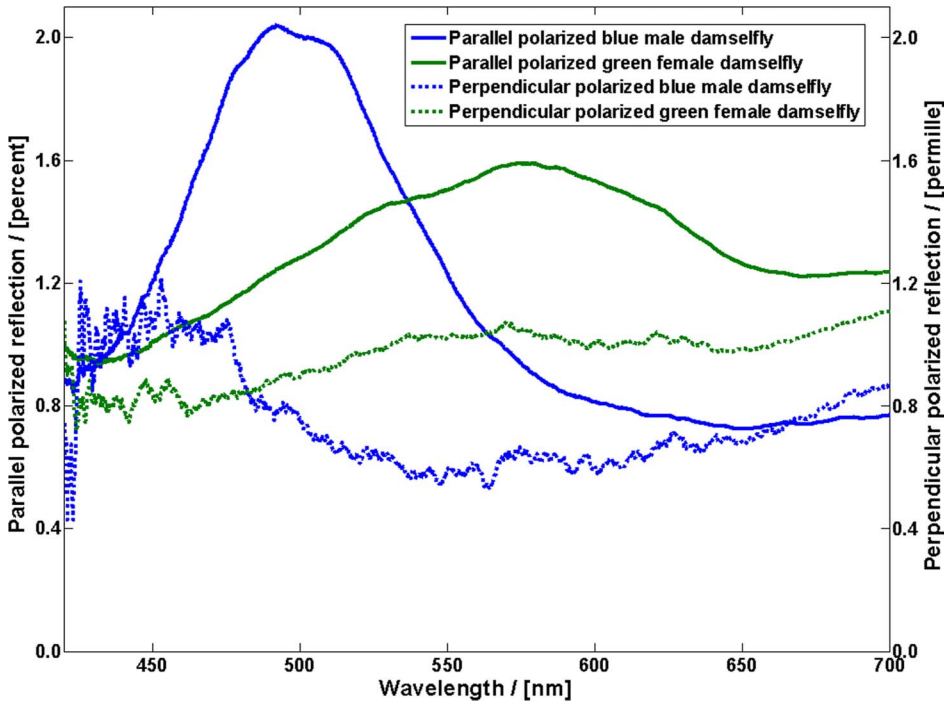

Fig. 4. (Color online) Polarized and depolarized whole-body reflectance measurements of *C. splendens* males and females. The blue and green reflectance features, respectively, disappear when polarizers are crossed. (Note the different scales.)

the specimen). The whole-body reflectances in Fig. 4 were also measured at a 15° angle with respect to the illumination. Further angular studies (data not presented here) reveal that the specimens have strong retroreflective properties, and that most light is reflected back directly toward the illumination. Also, the structural features are displaced to lower wavelengths when the angle between illumination and observation increases (shifts of the order of 50 nm were observed over 60°). This might have biological relevance, since the appearance to aquatic predators would be more bluish and match the sky, while the appearance to terrestrial predators would be slightly more greenish and match the vegetation.

Since broadband reflectance time-resolved lidar is labor intensive to perform, considering requirements for pulsed collimated sources, it would be considerably more realistic to perform LIF lidar. For this reason, the resemblance of reflectance and fluorescence was studied. It is well known that fluorescence spectroscopy cannot be performed without the influence of reflectance and transmission or considering photon migration spectroscopy. Thus, we can expect certain correlations between the two methods. Dried *C. splendens* specimens were measured at several spots using a bifurcated fiber probe; see Fig. 5. The illuminating fiber was connected to a diode laser at 375 nm (Power Technology Incorporated) or a white-light xenon flash (Ocean Optics, PX-2) for fluorescence and reflectance measurements, respectively. The collected light was detected in a spectrometer (Ocean Optics, USB4000) through a GG400 long-pass filter [75]. The sample and probe remained fixed at a 5 mm distance from the target in the fluorescence and reflectance measurements.

It is a general phenomenon that shorter excitation wavelengths are typically absorbed in the outer layers of biological samples [49,67] and autofluorescence from a number of biological compounds is usually produced with a small Stokes shift and with broad bluish–greenish fluorescence spectra. The measurements were performed at various spots on the specimens; however, not all data are presented here. Both laboratory and lidar test-range measurements suggest that bluish reflecting samples appear even more bluish under fluorescence, and greenish reflecting samples appear even more greenish under fluorescence; see Fig. 6. Our current understanding is that excitation light is absorbed in the outer layers of the cuticulum, either by wax, melanin, chitin, or in the scattering nanospheres themselves, producing broadband fluorescence light, which, in turn, is reflected by the underlying structural color-generating layers. In this way, the structural color enhances the blue or the green part of the fluorescence that is produced.

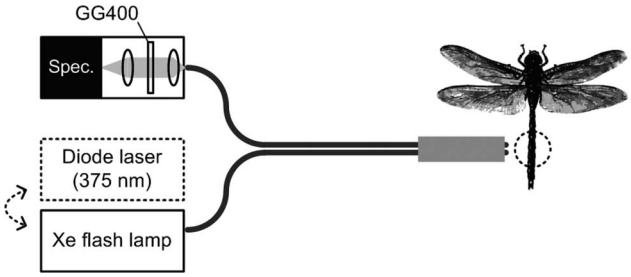

Fig. 5. Setup for fiber point measurements. Either a UV laser line or white light is passed into the bifurcated probe. The sample geometry is maintained constant between the measurements. A long-pass GG400 filter prevents blooming in the spectrometer (Spec.).

B. Lidar Test-Range Measurements

The Lund mobile lidar system, which is thoroughly described in [7] and displayed in Fig. 7, was used for remote measurements on damselflies. It is basically a coaxial system with a Ø 40 cm vertically looking telescope with the optical path folded by a roof-top scanning mirror. The repetition rate is 20 Hz. One laser transmitter is a *Q*-switched Nd:YAG laser, where the fundamental (1064 nm), the second-harmonic (532 nm), the third (355 nm), and the forth-harmonic (266 nm) frequencies can be produced simultaneously. A second transmitter is a Nd:YAG-pumped optical parametric oscillator (OPO) system with wide

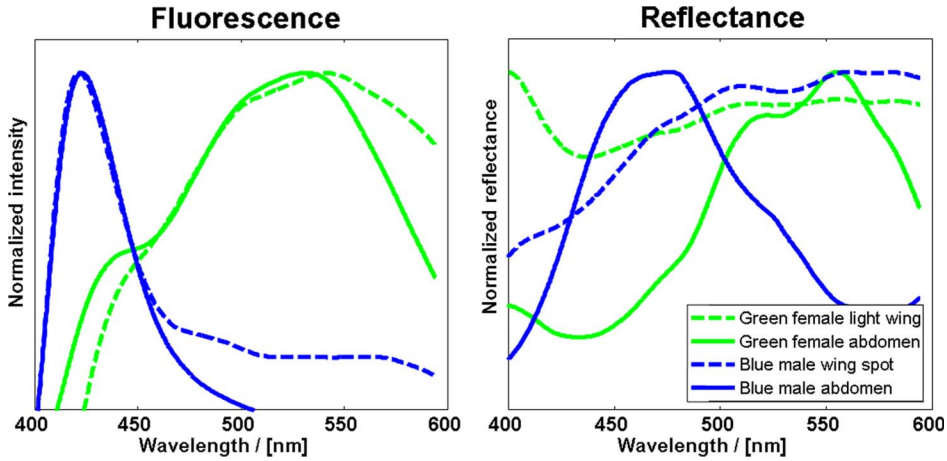

Fig. 6. (Color online) Comparison between reflectance and fluorescence spectra. In general, all measurements performed in this study suggest a positive correlation between fluorescence emission and reflectance.

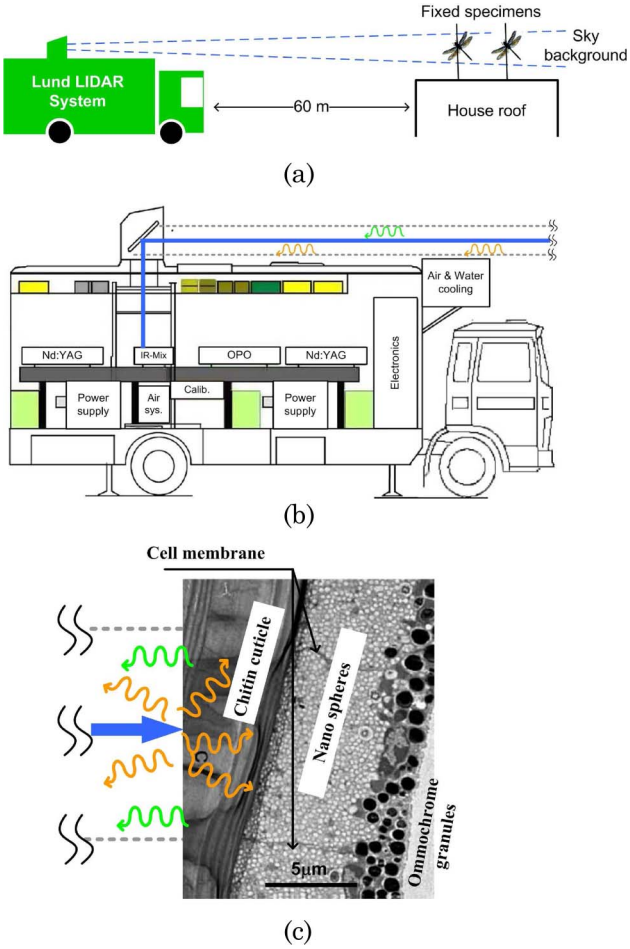

Fig. 7. (Color online) (a) Setup for test-range experiments. Insects were mounted on thin clean aluminum threads and were detected toward a bright sky background. (b) The versatile mobile lidar provides pulsed light continuously from 200 nm to 4 μm. (c) The UV laser light induces broad fluorescent light in the wax or chitin, which is, in turn, partly reflected in the nanosphere array.

tunability, augmented by nonlinear wavelength-shifting techniques. In our initial experiments, we employed only the 355 and 266 nm radiation for demonstration. In the measurements, the pulse energies are limited to 25 and 10 mJ, respectively, for these two wavelengths. The FWHM of the laser pulse is approximately 15 ns, corresponding to about 2.25 m axial resolution. The spot size for the test-range measurements of targets at 60 m was approximately Ø 10 cm. For the time-domain recording, a photomultiplier tube (PMT) (EMI 9816 QA) was used as the detector and an oscilloscope (Tektronix TDS544B) was used as the digitizer, sampling every 4 ns. The elastic signal was recorded through a 45° 355 nm dichroic mirror followed by a Schott UG11 filter to further suppress the background. Two fluorescence bands were recorded simultaneously by additional PMTs but will not be presented in this paper. For initial remote spectral analysis of LIF, an intensified fiber-coupled optical multiple channel analyzer (OMA) system is employed. With a 1 mm diameter fiber to transport light from the telescope focal plane to the spectrometer, and using the fiber end as the "slit," a spectral resolution of 14 nm was obtained. Detailed information of the OMA system can be found in [76]. Fluorescence with excitation at 355 nm was detected from the 60 m distant target through a 5 mm GG400 Schott filter, and fluorescence with excitation at 266 nm was detected though a 3 mm WG305 Schott filter; in each case the filters were used to suppress the overwhelming elastic signal while transmitting fluorescence at the lowest wavelengths as possible.

Elastic lidar returns from damselflies, which are mounted at 60 and 80 m distances, are shown in Fig. 8. Pulses at the third-harmonic Nd:YAG wavelength, 355 nm, were sent out after initial expansion into a 5 cm diameter beam, and echoes were collected with the lidar telescope. Elastic photons were selected with a diachroic 45° laser line mirror followed by a Schott UG11 high-pass glass filter. The signal was recorded by the PMT. Measurements were performed on two dried specimens of *C. splendens*, exposed to the expanded laser beam and with the gray sky as the background. The damselflies were held by thin aluminum wires (echoes from the wires were relatively small). The orientation and the position of the two specimens in the beam were heavily randomized by high wind speeds. Apart from the strong reflection from the window of the lidar system, both specimens are clearly resolved. The second echo is slightly weaker than the first. This might be explained by different orientation and positions in respect to the beam; also, the first specimen is partly shadowing both excitation and backscattered photons. Also, the trivial LIDAR signal falloff with range is at play.

Results from fluorescence measurements with the OMA system are shown in Fig. 9, for 355 and 266 nm excitation. Slight differences between the genders of *C. splendens* can be seen. The autofluorescence spectra were recorded at a 60 m distance at 355 nm excitation and in the lidar laboratory at 266 nm excitation (due to weather conditions). The insect specimens were the same. but the orientation was random as before. Beam sizes were Ø 10 cm and 1 cm, respectively. A GG400 and a WG305 Schott long-pass filter

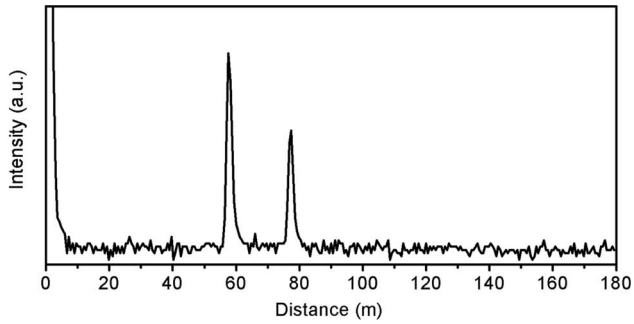

Fig. 8. Elastic lidar recording of mounted damselflies; the transmitted wavelength is 355 nm. Data are from a single laser pulse and the echoes arises from two fixed specimens (*C. splendens* female and male respectively) separated by 20 m. Fluorescence time series recording were also performed but are not presented in this paper.

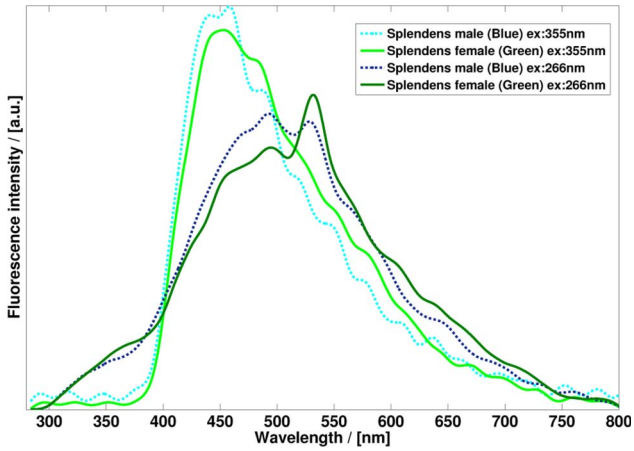

Fig. 9. (Color online) Normalized fluorescence spectra for 266 and 355 nm excitation; in both cases, imprints of the structural color are observed. Data from 20 laser shots were averaged.

were used, respectively. Emission spectra are broad and cover the region of 400–600 nm, where structural imprints are expected to occur. Emission spectra could be explained by previous measured spectra of both melanin and chitin. Even if the signal is weak, a slight difference between a blue and a green reflecting sample can be observed at both excitation wavelengths (Fig. 9). Both chitin and melanin absorption peak around 330 nm and the signal-to-noise ratio could probably be improved by moving to such an excitation wavelength.

Results of fluorescence lidar measurements on damselflies prepared with Coumarin 102 and Rhodamine 6G dye are shown in Fig. 10. In preparation for migration studies and population encoding experiments, dried specimens of both genders of *C. splendens* were sprayed with water solutions containing these dyes. Fluorescence spectra were measured at a 60 m distance with the same procedure as before. Apart from the obviously much stronger fluorescence signal from the two dyes, males and females with, respectively,

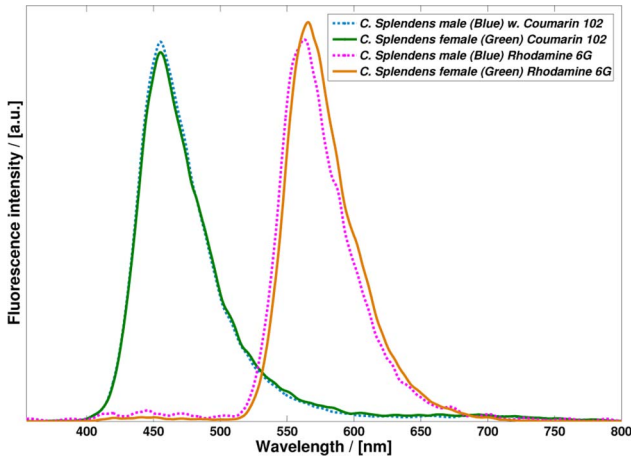

Fig. 10. (Color online) Fluorescence spectra for 355 nm excitation for dye-marked females and males of *C. splendens*. Strong dye fluorescence bands are seen with slight modifications due to structural colors. Data from 20 laser shots were averaged.

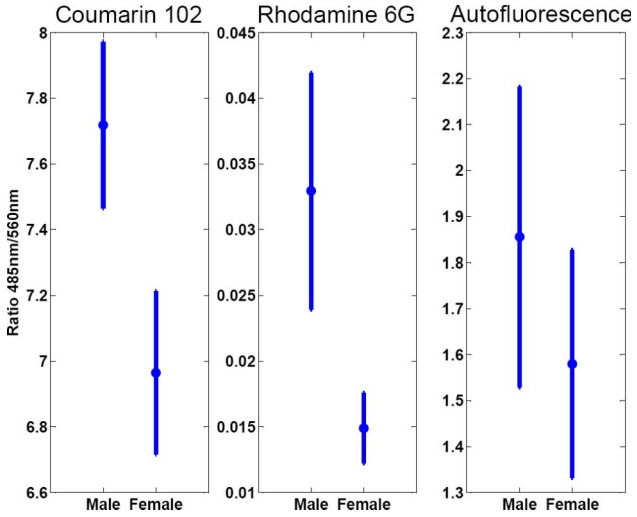

Fig. 11. *Calopteryx splendens* male/female contrast in autofluorescence and when using dye-enhanced fluorescence. Bars show standard deviation for a total of 20 shots. The overlap in autofluorescence is interpreted as lack of signal rather than lack of physical difference of the samples.

blue and green structural colors show distinct fluorescence spectra. This is in accordance with the view that the generated fluorescent light is reflected in the insect structures and, thus, the structural color imposes an imprint on the observed fluorescence.

Separation of male and female damselflies based on the measured ratio between two fluorescence intensities (at 485 and 560 nm, 25 nm FWHM, respectively) is illustrated in Fig. 11. In this case, we define the bands mathematically, with the spectra provided from the OMA, but such bands could easily by implemented using optical filters in front of PMTs with much higher sensitivity. When we take the ratio between the two bands, intensity units cancel, and the influence of all geometric effects due to sample orientation, position with respect to the laser beam, collection efficiencies, etc., cancel. We see a clear distinction between the *C. splendens* male and female specimens for the dyed samples. For the autofluorescence, the tendency is the same, but the contrast is poorer. This is mainly due to noisy signals rather than lack of physical differences.

4. Discussion

We have performed a feasibility study to investigate the possibilities of lidar to study interpopulation migration and movement of the damselfly species *Calopteryx splendens* and *C. virgo*. Laboratory, as well as testing-range measurements, of dried, mounted specimens at distances of 60 to 80 m were performed. The damselflies exhibit reflectance and fluorescence properties that are closely tied to the generation of structural colors. Laboratory measurements, including color photography in polarized light and spectroscopy of reflectance and induced fluorescence, revealed these phenomena and an interesting connection between reflectance and fluorescence features. To our knowledge, we are the first group to acquire

structural colors using lidar. The number of *C. virgo* samples was limited as the dried samples are considerably fragile; hence, they quickly disintegrate in the measurement wind conditions. Laboratory measurements on *C. virgo* involving polarized color photographing and point reflectance/fluorescence were carried out. The results of these measurements also confirmed that the reflectance is indeed largely influenced by nanostructures and, as for *C. splendens*, the emitted fluorescence is positively correlated with the reflectance at the same wavelength region. Studies on lidar data of *C. splendens* of both genders showed that males and females can be remotely distinguished, especially for specimens that were marked with the dyes Coumarin 102 and Rhodamine 6G. The strength of the fluorescence signals (when studied with an optical multichannel analyzer connected to the lidar telescope) indicated that an arrangement of a small number of PMTs, each detecting a chosen spectral band, is advantageous for realistic single-shot recordings of flying insects. With such a setup, range-resolved recordings are obtained, which is advantageous compared to the gated spectrometer approach, where the time gate has to be preset. Such an approach is now being implemented in preparation for upcoming field experiments, where damselflies in their natural habitat will be studied with the lidar beam positioned at different heights over the river surface. Field studies have the potential to bring new insights into the migration, movement, and flying patterns of *Calopteryx* damselflies, and will provide guidelines for studies of other insect species. One concern when using LIF lidar at 266 nm is the transmission of the excitation light in the atmosphere; depending on varying conditions, ozone absorption and air scattering will attenuate the excitation pulse. Early work experience from previous field campaigns tells us that lidar returns can be detected in horizontal soundings at kilometer ranges even at 254 nm, where ozone absorbs the most [77,78]. The conditions might, however, not always be feasible. Alternative solutions for acquisition of structural colors by lidar might be found in multiband illumination with several laser lines, or with pulsed supercontinuum light sources [79,80]. However, the issues concerning eye safety in field settings would be much more severe than for the eye-safe UV used in, e.g., LIF lidar.

This work was supported by a Swedish Research Council project grant and by a Linnaeus grant to the Lund Laser Centre, Sweden. Fruitful discussions with and kind help from Patrik Lundin, Richard Prum, Joseph A. Shaw, Eric Warrant, Erik Svensson, Lisa Orr, and Can Xu are gratefully acknowledged.

References

1. R. M. Measures, *Laser Remote Sensing: Fundamentals and Applications* (Wiley, 1984).
2. R. M. Measures, ed., *Laser Remote Chemical Analysis* (Wiley-Interscience, 1988).
3. M. Sigrist, ed., *Air Pollution Monitoring with Optical Techniques* (Wiley, 1993).
4. C. Weitkamp, ed., *LIDAR: Range-Resolved Optical Remote Sensing of the Atmosphere*, Springer Series in Optical Sciences (Springer, 2005).
5. T. Fujii and T. Fukuchi, eds., *Laser Remote Sensing* (CRC, 2005).
6. S. Svanberg, "LIDAR," in *Springer Handbook of Lasers and Optics* F. Träger, ed. (Springer, 2007), pp. 1031–1052.
7. P. Weibring, H. Edner, and S. Svanberg, "Versatile mobile lidar system for environmental monitoring," Appl. Opt. **42**, 3583–3594 (2003).
8. S. Harsdorf, M. Janssen, R. Reuter, B. Wachowic, and R. Willkomm, "Lidar as part of an ROV-based sensor network for the detection of chemical pollutants on the seafloor," in *Oceans '98 Conference Proceedings* (IEEE, 1998), Vol. 3, pp. 1250–1253.
9. M. Sowinska, B. Cunin, F. Heisel, and J. A. Miehé, "New UV-A laser-induced fluorescence imaging system for near-field remote sensing of vegetation: characteristics and performances," Proc. SPIE **3707**, 91–102 (1999).
10. D. M. Winker, C. A. Hostetler, M. A. Vaughan, and A. H. Omar, "Mission, Instrument, and Algorithms Overview," PC-SCI-202.01 (NASA, 2006), www-calipso.larc.nasa.gov.
11. J. A. Shaw, N. L. Seldomridge, D. L. Dunkle, P. W. Nugent, L. H. Spangler, J. J. Bromenshank, C. B. Henderson, J. H. Churnside, and J. J. Wilson, "Polarization lidar measurements of honey bees in flight for locating land mines," Opt. Express **13**, 5853–5863 (2005).
12. S. Svanberg, "Laser fluorescence spectroscopy in environmental monitoring," in *Optoelectronics for Environmental Science*, S. Martellucci and A. N. Chester, eds. (Plenum 1990), pp. 15–27.
13. H. Edner, J. Johansson, S. Svanberg, and E. Wallinder, "Fluorescence lidar multicolor imaging of vegetation," Appl. Opt. **33**, 2471–2479 (1994).
14. P. Weibring, Th. Johansson, H. Edner, S. Svanberg, B. Sundnér, V. Raimondi, G. Cecchi, and L. Pantani, "Fluorescence lidar imaging of historical monuments," Appl. Opt. **40**, 6111–6120 (2001).
15. S. Svanberg, "Fluorescence spectroscopy and imaging of LIDAR targets," in *Laser Remote Sensing*, T. Fujii and T. Fukuchi eds. (CRC, 2005), Chap. 6.
16. Ø. Farsund, G. Rustad, I. Kåsen, and T. V. Haavardsholm, "Required spectral resolution for bioaerosol detection algorithms using standoff laser induced fluorescence measurements," IEEE Sens. J. **6** (2009).
17. D. N. Whiteman, S. H. Melfi, and R. A. Ferrare, "Raman LIDAR system for the measurement of water-vapor and aerosols in the earths atmosphere," Appl. Opt. **31**, 3068–3082 (1992).
18. V. E. Zuev, Y. D. Kopytin, V. A. Korolkov, M. E. Levitskii, M. F. Nebolsin, B. G. Sidorov, and N. P. Soldatkin, in *Proceedings of the 13th International Laser Radar Conference* (NASA Langley Research Center, 1986).
19. S. Palanco, J. M. Baena, and J. J. Laserna, "Open-path laser-induced plasma spectrometry for remote analytical measurements on solid surfaces," Spectrochim. Acta B **57**, 591–599 (2002).
20. K. Stelmaszczyk, P. Rohwetter, G. Méjean, J. Yu, E. Salmon, J. Kasparian, R. Ackermann, J.-P. Wolf, and L. Wöste, "Long-distance remote laser-induced breakdown using filamentation in air," Appl. Phys. Lett. **85**, 3977–3979 (2004).
21. R. Grönlund, M. Lundqvist, and S. Svanberg, "Remote imaging laser-induced breakdown spectroscopy and laser-induced fluorescence spectroscopy using nanosecond pulses from a mobile lidar system," Appl. Spectrosc. **60**, 853–859 (2006).
22. T. Fujii, N. Goto, M. Miki, T. Nayuki, and K. Nemoto, "Lidar measurement of constituents of microparticles in air by

laser-induced breakdown spectroscopy using femtosecond terawatt laser pulses," Opt. Lett. **31**, 3456–3458 (2006).
23. M. Skolnik, *Introduction to Radar Systems*, 3rd ed. (McGraw-Hill, 2002).
24. J. C. Toomay and P. J. Hannen, *Radar Principles for the Non-Specialist*, 3rd ed. (SciTech, 2004).
25. S. A. Gauthreaux Jr. and C. G. Belser, "Radar ornithology and biological conservation," The Auk **120**, 266–277 (2003).
26. J. W. Chapman, D. R. Reynolds, and A. D. Smith, "Vertical-looking radar: a new tool for monitoring high-altitude insect migration," BioScience **53**, 503–511 (2003).
27. D. T. Gjessing, *Target Adaptive Matched Illumination Radar: Principles and Applications* (Institution of Engineering and Technology, 1986).
28. S. P. Lohmeier, S. M. Sekelsky, J. M. Firda, G. A. Sadowy, and R. E. McIntosh, "Classification of particles in stratiform clouds using the 33 and 95 GHz polarimetric cloud profiling radar system (CPRS)," IEEE Trans. Geosci. Remote Sens. **35**, 256–270 (1997).
29. K. Fredriksson, B. Galle, K. Nyström, S. Svanberg, and B. Öström, "Underwater laser-radar experiments for bathymetry and fish-school detection," Göteborg Institute of Physics Reports GIPR-162 (Chalmers University of Technology, Göteborg, 1978).
30. K. Fredriksson, B. Galle, K. Nyström, S. Svanberg, and B. Öström, "Marine laser probing: results of a field test," Meddelanden från Havsfiskelaboratoriet No. 245 (Swedish Department of Fishery, Stockholm, 1979).
31. K. S. Repasky, J. A. Shaw, R. Scheppele, C. Melton, J. L. Carsten, and L. H. Spangler, "Optical detection of honeybees by use of wing-beat modulation of scattered laser light for locating explosives and land mines," Appl. Opt. **45**, 1839–1843 (2006).
32. D. S. Hoffman, A. R. Nehrir, K. S. Repasky, J. A. Shaw, and J. L. Carlsten, "Range-resolved optical detection of honeybees by use of wing-beat modulation of scattered light for locating land mines," Appl. Opt. **46**, 3007–3012 (2007).
33. Von R. Bloch, B. Bruderer, and P. Steiner, "Flugverhalten nächtlich ziehender Vögel—Radardaten über den Zug verschiedener auf einem Alpenpass," Die Vodelwarte **31**, 119–146 (1981).
34. P. S. Corbet, *Behavior and Ecology of Odonata* (Harley, 1999).
35. M. Campero, F. Ollevier, and R. Stoks, "Ecological relevance and sensitivity depending on the exposure time for two biomarkers," Environ. Toxicol. **22**, 572–581 (2007).
36. C. A. Deutsch, J. J. Tewksbury, R. B. Huey, K. S. Sheldon, C. K. Ghalambor, D. C. Haak, and P. R. Martin, "Impacts of climate warming on terrestrial ectotherms across latitude," Proc. Natl. Acad. Sci. USA **105**, 6668–6672 (2008).
37. C. Parmesan, "Ecological and evolutionary responses to recent climate change," Annu. Rev. Ecol. Evol. Syst. **37**, 637–669 (2006).
38. C. N. Parmesan, C. Ryrholm, C. Steganescu, J. K. Hill, C. D. Thomas, B. Descimon, B. Huntley, L. Kaila, J. Kullberg, T. Tammaru, W. J. Tennent, J. A. Thomas, and M. Warren, "Poleward shifts in geographical ranges of butterfly species associated with regional warming," Nature **399**, 579–583 (1999).
39. R. Hickling, D. B. Roy, J. K. Hill, and C. D. Thomas, "A northward shift of range margins in British Odonata," Glob. Change Biol. **11**, 502–506 (2005).
40. T. J. Case and M. L. Taper, "Interspecific competition, environmental gradients, gene flow, and the coevolution of species' borders," Am. Nat. **155**, 583–605 (2000).
41. D. Garant, S. E. Forde, and A. P. Hendry, "The multifarious effects of dispersal and gene flow on contemporary adaptation," Funct. Ecol. **21**, 434–443 (2007).
42. J. R. Hagler and C. G. Jackson, "Methods for marking insects: current techniques and future prospects," Annu. Rev. Entomol. **46**, 511–543 (2001).
43. M. D. Ginzel and L. M. Hanks, "Evaluation of synthetic hydrocarbons for mark–recapture studies on the red milkweed beetle," Journal of chemical ecology **28**, 1037–1043 (2002).
44. R. W. Piper, "A novel technique for the individual marking of smaller insects," Entomol. Exper. Appl. **106**, 155–157 (2003).
45. A. E. A. Stephens, A. M. Barrington, V. A. Bush, N. M. Fletcher, V. Mitchell, and J. D. M. Suckling, "Evaluation of dyes for marking painted apple moths (*Teia anartoides Walker, Lep. Lymantriidae*) used in a sterile insect release program," Aust. J. Entomol. **47**, 131–136 (2008).
46. T. P. Gosden and E. I. Svensson, "Density-dependent male mating harassment, female resistance and male mimicry," Am. Nat. **173**, 709–721 (2009).
47. L. Celander, K. Fredriksson, B. Galle, and S. Svanberg, "Investigation of laser-induced fluorescence with applications to remote sensing of environmental parameters," Göteborg Institute of Physics Reports GIPR-149 (Chalmers University of Technology, Göteborg 1978).
48. T. D. Schultz, C. N. Anderson, and L. B. Symes, "The conspicuousness of colour cues in male pond damselflies depends on ambient light and visual system," Anim. Behav. **76**, 1357–1364 (2008).
49. H. Edner, J. Johansson, S. Svanberg, E. Wallinder, M. Bazzani, B. Breschi, G. Cecchi, L. Pantani, B. Radicati, V. Raimondi, D. Tirelli, G. Valmori, and P. Mazzinghi, "Laser-induced fluorescence monitoring of vegetation in Tuscany," EARSeL Adv. Remote Sens. **1**, 119–130 (1992).
50. G. Rüppel, D. Hilfert-Rüppel, G. Rehfeldt, and C. Schütte, *Die Prachtlibellen Europas*, Die neue Brehm-Bücherei Bd. 654 (Westarp Wissenschaften, 2005).
51. Lord Rayleigh, "The iridescant colours of birds and insects," Proc. R. Soc. A Biol. Sci. **128**, 624–641 (1930).
52. M. Srinivasarao, "Nano-optics in the biological world: beetles, butterflies, birds, and moths," Chem. Rev. **99**, 1935–1961 (1999).
53. A. R. Parker and N. Martini, "Structural colour in animals—simple to complex optics," Opt. Laser Technol. **38**, 315–322 (2006).
54. S. Kinoshita, S. Yoshioka, Y. Fujii, and N. Okamoto, "Photophysics of structural color in the morpho butterflies," Forma **17**, 103–121 (2002).
55. P. Vukusic, J. R. Sambles, and C. R. Lawrence, "Structurally assisted blackness in butterfly scales," Proc. R. Soc. Biol. Sci. **271**, 237–239 (2004).
56. P. Vukusic, J. R. Sambles, C. R. Lawrence, and R. J. Wootton, "Now you see it—now you don't," Nature **410**, 36 (2001).
57. I. R. Hooper, P. Vukusic, and R. J. Wootton, "Detailed optical study of the transparent wing membranes of the dragonfly Aeshna cyanea," Opt. Express **14**, 4891–4897 (2006).
58. J. A. Noyes, P. Vukusic, and I. R. Hooper, "Experimental method for reliably establishing the refractive index of buprestid beetle exocuticle," Opt. Express **15**, 4351–4358 (2007).
59. V. Backman, R. Gurjar, K. Badizadegan, I. Itzkan, R. R. Dasari, L. T. Perelman, and M. S. Feld, "Polarized light scattering spectroscopy for quantitative measurement of epithelial cellular structures *in situ*," IEEE J. Sel. Top. Quantum Electron. **5**, 1019–1026 (1999).
60. T. Wagner, S. Beirle, T. Deutschmann, M. Grzegorski, and U. Platt, "Satellite monitoring of different vegetation types by differential optical absorption spectroscopy (DOAS) in the red spectral range," Atmos. Chem. Phys. **7**, 69–79 (2007).
61. R. O. Prum, J. A. Cole, and R. H. Torres, "Blue integumentary structural colours in dragonflies (*Odonata*) are not produced by incoherent Tyndall scattering," J. Exp. Biol. **207**, 3999–4009 (2004).

62. S. Fizeau-Braesch, "Pigments and color changes," Annu. Rev. Entomol. **17**, 403–424 (1972).
63. J. M. Gallas and M. Eisner, "Fluorescence of melanin—dependence upon excitation wavelength and concentration," Photochem. Photobiol. **45**, 595–600 (1987).
64. G. Luna-Bárcenas, B. Gonzalez-Campos, E. A. Elizalde-Peña, E. Vivaldo-Lima, J. F. Louvier-Hernández, Y. V. Vorobiev, and J. González-Hernández, "FEMO modelling of optical properties of natural biopolymers chitin and chitosan," Phys. Stat. Sol. **5**, 3736–3739 (2008).
65. L. Q. Wu, R. Ghodssi, Y. A. Elabd, and G. F. Payne, "Biomimectic pattern transfer," Adv. Funct. Mater. **15**, 189–195 (2005).
66. S. N. Gorba, A. Keselb, and J. Bergera, "Microsculpture of the wing surface in *Odonata*: evidence for cuticular wax covering," Arthropod Struct. Dev. **29**, 129–135 (2000).
67. A. Ounis, Z. G. Cerovic, J. M. Briantais, and I. Moya, "DEFLIDAR: a new remote sensing instrument for estimation of epidermal UV absorption in leaves and canopies," in *Proceedings of European Association of Remote Sensing Laboratories (EARSeL)-SIG-Workshop LIDAR, Dresden/FRG* (EARSeL, 2001), Vol. 1, pp. 196–204.
68. J. F. Jacobs, G. J. M. Koper, and W. N. J. Ursem, "UV protective coatings: a botanical approach," Prog. Org. Coatings **58**, 166–171 (2007).
69. E. Warrant, ed., *Invertebrate Vision* (Cambridge U. Press, 2006).
70. M. Wellereuther, M. Brydegaard, and E. Svensson are preparing a manuscript called "Role of female wing colour and male mate choice in premating isolation in allopatric and sympatric populations of damselflies".
71. G. De Marchi, "Precopulatory reproductive isolation and wing colour dimorphism in *Calopteryx splendens* females in southern Italy *(Zygoptera: Calopterygidae)*," Odonatologica **19**, 243–250 (1990).
72. M. J. Rantala, J. Koskimäki, J. Suhonen, J. Taskinen, and K. Tynkkynen, "Immunocompetence, developmental stability and wing spot size in *Calopteryx splendens*," Proc. R. Soc. B **267**, 2453–2457 (2000).
73. E. I. Svensson, L. Kristoffersen, K. Oskarsson, and S. Bensch, "Molecular population divergence and sexual selection on morphology in the banded demoiselle (*Calopteryx splendens*)," Heredity **93**, 423–433 (2004).
74. K. Tynkkynen, J. S. Kotiaho, M. Luojumäki, and J. Suhonen, "Interspecific territoriality in *Calopteryx* damselflies: the role of secondary sexual characters," Anim. Behav. **71**, 299–306 (2006).
75. U. Gustafsson, S. Pålsson, and S. Svanberg, "Compact fiber-optic fluorosensor using a continuous-wave violet diode laser and an integrated spectrometer," Rev. Sci. Intrum. **71**, 3004–3006 (2000).
76. C. af Klinteberg, M. Andreasson, O. Sandström, S. Andersson-Engels, and S. Svanberg, "Compact medical fluorosensor for minimally invasive tissue characterization," Rev. Sci. Instrum. **76**, 034303 (2005).
77. H. Edner, P. Ragnarson, S. Svanberg, E. Wallinder, R. Ferrara, B. E. Maserti, and R. Bargagli, "Atmospheric mercury mapping in a cinnabar mining area," Sci. Total Environ. **133** 1–15 (1993).
78. E. Wallinder, H. Edner, P. Ragnarson, and S. Svanberg, "Vertically sounding ozone LIDAR system based on a KrF excimer laser," Phys. Scr. **55**, 714–718 (1997).
79. C. af Klinteberg, A. Pifferi, S. Andersson-Engels, R. Cubeddu, and S. Svanberg, "In vivo absorption spectroscopy of tumor sensitizers using femtosecond white light," Appl. Opt. **44**, 2213–2220 (2005).
80. Ch. Abrahamsson, T. Svensson, S. Svanberg, S. Andersson-Engels, J. Johansson, and S. Folestad, "Time and wavelength resolved spectroscopy of turbid media using light continuum generated in a crystal fibre," Opt. Express **12**, 4103–4112 (2004).